J Mater Sci (2011) 46:1844–1849
DOI 10.1007/s10853-010-5011-5

Preparation and characterization of olivary carbon by pyrolysis of ethanol with the manganese acetate as promoter via solvothermal method

Wenqi He · Yong Xiao · Jialiang Cheng · Guandong Wei · Shuai Zhao · Guangui Yi · Yingliang Liu

Received: 21 July 2010 / Accepted: 15 October 2010 / Published online: 26 October 2010

Abstract A new single step, efficient, and scalable process was developed for synthesis of olivary carbon microparticles with a diameter of 4–6 μm at the middle and a length 8–12 μm by pyrolysis (under 600 °C) of ethanol with manganese acetate as the promoter. The physical and chemical structures of the olivary carbon were investigated by X-ray powder diffraction, scanning and transmission electron microscopy and Fourier transform infrared spectroscopy. The content of the olivary carbon in the product is related to the pyrolysis temperature, the reaction time, and the dosage of the promoter. The content of the olivary carbon was over 90% of the product under the optimum condition. A possible formation process of the olivary carbon has been put forward according to the experimental data available.

Introduction

Since the synthesis of molecular carbon structures in the form of C_{60} and other fullerenes in 1985 [1], carbon materials have attracted more and more attention. Considerable efforts have been made on the preparation, growth mechanism, and application of carbon materials. Arc discharge [2], laser ablation [3] chemical vapor deposition (CVD) [4], and hydrothermal processing [5, 6] were used to synthesize carbon material. And the solvothermal technique [7] was developed based on the hydrothermal technique, which was widely used in the synthesis of carbon materials for the advantages of the flexible experiment conditions, simple operation, and low cost. Many types of carbon materials have been synthesized in this way, such as carbon spheres [8], hollow carbon spheres [9], hollow carbon cones [10], all kinds of carbon nanotubes [11–14], iron/carbon core–shell coaxial nanocables [15], straw-like carbon microbundles [16], flower-like carbon [17] and so on.

More recently, nonspherical carbon materials may be more attractive in applications than the spherical because of their low symmetries. And it is worth finding different ways to synthesize nonspherical carbon materials. Several results have been reported about the preparation of olivary carbon, which is a novel nonspherical carbon material with olive-like morphology. Luo et al. [18] have synthesized olivary carbon by pyrolysis of acetone with metallic zinc as the catalyst at 600 °C. Ma et al. [19] synthesized monodispersed olivary carbon microparticles with copper as substrate-assisted. Lately, Pol et al. [20] had reported a synthesis method of olivary-shaped carbon from olive oil just through one step and catalyst-free. However, there remains still a blank as to the mechanism of detailed formation of olivary carbon.

In this manuscript, we synthesized mono-dispersed olivary carbon microparticles on a large-scale by using absolute ethanol and manganese acetate as solvent and promoter. We demonstrate a new single step, efficient and scalable solvothermal process for synthesis of olivary carbon, and the yield was up to 90%. The pyrolysis temperature, the reaction time, and the dosage of the promoter we adopted were investigated. And a new possible schematic illustration for the formation of the olivary carbon microparticles has been put forward and discussed.

W. He · Y. Xiao · J. Cheng · G. Wei · S. Zhao · G. Yi · Y. Liu (✉)
Department of Chemistry and Institute of Nanochemistry, Jinan University, Guangzhou 510632, People's Republic of China
e-mail: tliuyl@jnu.edu.cn

Experimental section

All reagents were commercially available and used without further purification. In a typical experiment, 1.5 g Mn $(CH_3COO)_2{\cdot}4H_2O$ was dissolved in 40 mL absolute ethanol completely, and then the solution was devolved into a 60 mL stainless steel autoclave. After being sealed, the autoclave was heated from room temperature to 600 °C (10 °C/min) and maintained at 600 °C for 12 h, then cooled down to room temperature naturally. The loose dark product was collected, dipped in dilute hydrochloric acid for 24 h, then filtered and washed by distilled water and absolute ethanol, last dried in a vacuum at 60 °C for 6 h.

Structural characterization was performed by using X-ray powder diffraction (XRD) (Brucks D8 X-ray powder diffractometer, CuKα radiation $\lambda = 1.541874$ Å). The morphologies of the samples were characterized with scanning electron microscopy (SEM, Philips XL-30s) and transmission electron microscopy (TEM, Philips Tecnai-10). Thermal gravimetric analysis (TGA) was taken on a SDT-Q600 thermal analyzer under N_2 flow. Fourier transform infrared (FTIR) spectra were recorded on an EQUINOX 55 (Bruker) spectrometer.

Results and discussion

Figure 1 gives the XRD patterns of the as-prepared products before and after the treatment by dilute HCl. According to index JCPDS Card File No. 01-083-1763, the starting material of Mn $(CH_3COO)_2{\cdot}4H_2O$, under the given reaction condition, was decomposed to form rhombohedral $MnCO_3$ (see curve a in Fig. 1). The diffraction planes of hexagonal graphite are showed in curve b. The broad peak

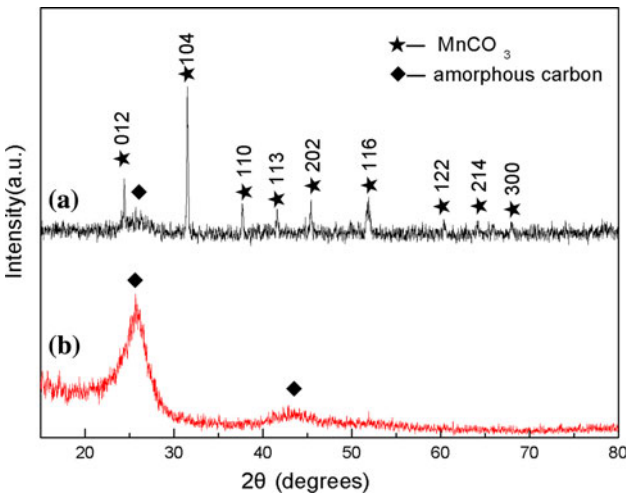

Fig. 1 XRD patterns of the products before *a* and after *b* HCl treatment

at around 26° could be attributed to the (002) diffraction planes, and another peak at around 43° corresponds to the (101) plane of graphite (JCPDS Card File No. 41-1487). The two peaks indicate that the product has a low graphitic degree; the olivary carbon is amorphous carbon phase.

The SEM image in Fig. 2a exhibits uniform olivary carbon of the as-prepared products and indicates most of the carbon particles are regular olivary, except a few have defect. It can also be seen in Fig. 2a that the olivary carbon particles with a diameter of 4–6 μm at the middle and a length 8–12 μm, and the content of the olivary carbon particles was estimated over 90% of the product. The solid nature of the olivary carbon is confirmed by the TEM image (Fig. 2b) and higher magnification image of half-particle (Fig. 2c). The olivary carbon has a smooth surface, but we also find some fragments around it. The SEM image in Fig. 2d shows the fragment under higher magnification, which plays an important role in the formation of the olivary carbon; we will give a further discussion in the mechanism.

The effects of the reaction temperature and time on the formation of the olivary carbon were investigated. We have found that the optimal reaction temperature was 600 °C, and no olivary carbon was produced when the temperature was below 500 °C. We carried out comparative experiments adopted 1.5 g $Mn(CH_3COO)_2{\cdot}4H_2O$ and found out that reaction time strongly affect the yield of olivary carbon. Figure 3a is the SEM image of the sample obtained by pyrolysis of ethanol maintained at 600 °C for 2 h, in addition to some nonuniform carbon spheres (the diameter of the bigger ones are about 4–6 μm, and the lesser ones are about 1–3 μm), we do not see olivary carbon. When the reaction time was extended to 5 h (Fig. 3b), a few carbon spheres have grown into olivary carbon from nonuniform carbon spheres, and the reaction time of 12 h gave the largest quantity of the olivary carbon. When the reaction was maintained at 600 °C for 24 h, nonuniform carbon spheres fully changed into olivary carbon seen from Fig. 3d, but some fused together. The experiment results showed that 2 h was not enough to form olivary carbon, and the perfect morphology couldn't be kept when the time extended to 24 h, so 12 h was considered as the optimal reaction time.

In order to investigate the role of manganese acetate in the process, a series of experiments have been done. Different amounts of $Mn(CH_3COO)_2{\cdot}4H_2O$ (0.1, 0.5, 1.5, and 3.0 g) was dissolved in 40 mL ethanol and other experiment conditions unchanged. Figure 4a gives the SEM image of the sample by pyrolysis of ethanol without manganese acetate. Many carbon spheres and a few olivary particles can be seen in Fig. 4a, which indicates that ethanol has a self-orientation to form olivary morphology in the process of pyrolysis. Comparing the images in Figs. 3c

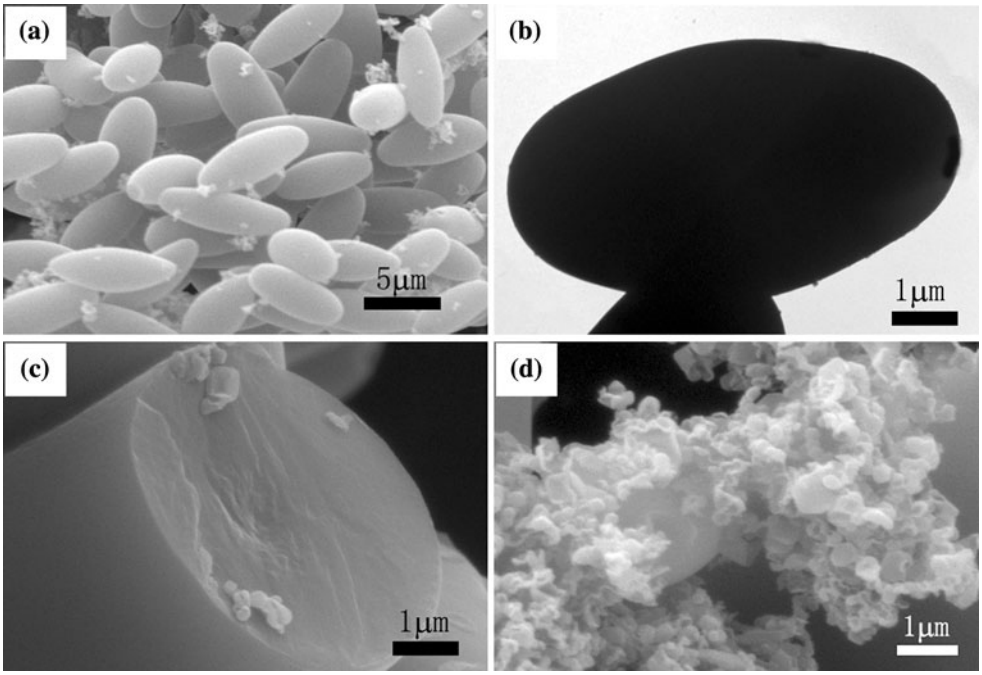

Fig. 2 **a** SEM image of the olivary carbon, **b** TEM image of a single olivary carbon, **c** high-resolution SEM image of the olivary carbon half-particles, and **d** SEM image of the carbon fragment under higher magnification

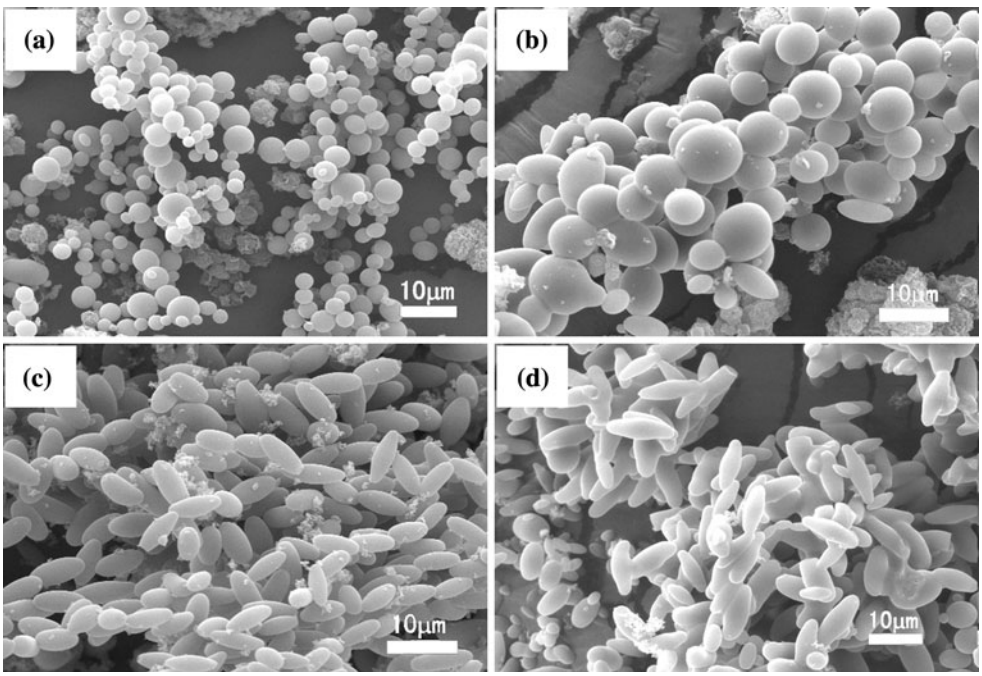

Fig. 3 SEM images of the samples obtained by pyrolysis of ethanol maintained at 600 °C for different reaction time: **a** 2 h, **b** 5 h, **c** 12 h, and **d** 24 h

and 4b–e, we have found that with the increase of the amount of $Mn(CH_3COO)_2{\cdot}4H_2O$, the content of the olivary particles are increasing, and the morphology of the olivary particles become uniform and pretty. At the same time, the amount of the carbon fragment was increasing with the augment of the $Mn(CH_3COO)_2{\cdot}4H_2O$. With the set of experiments, the results show that manganese acetate plays a vital role in the formation of olivary carbon, and 1.5 g $Mn(CH_3COO)_2{\cdot}4H_2O$ was selected as the optimum condition.

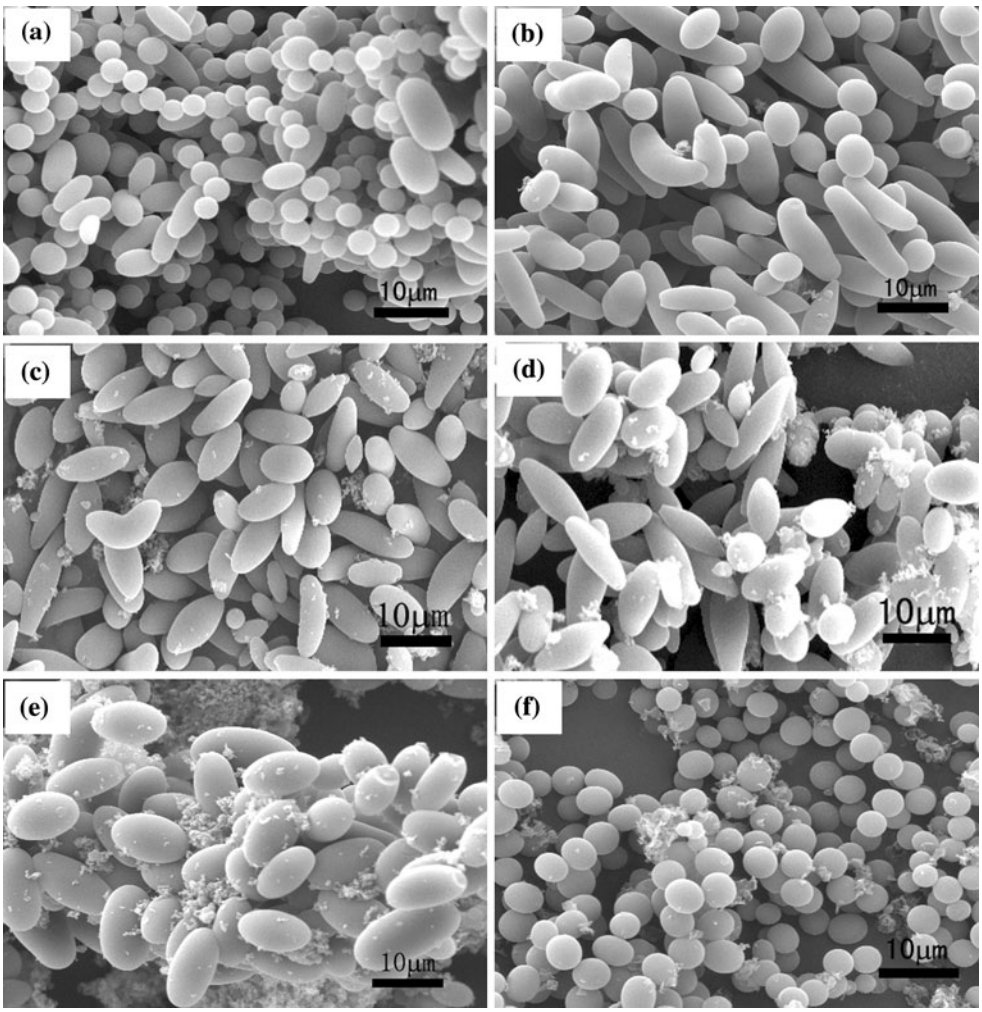

Fig. 4 SEM images of the samples obtained by pyrolysis of ethanol at 600 °C for 12 h with different amounts of promoter: **a** none, **b** 0.1 g $Mn(CH_3COO)_2{\cdot}4H_2O$, **c** 0.5 g $Mn(CH_3COO)_2{\cdot}4H_2O$, **d** 1.0 g $Mn(CH_3COO)_2{\cdot}4H_2O$, **e** 3.0 g $Mn(CH_3COO)_2{\cdot}4H_2O$, and **f** 1.5 g $MnCO_3$

To determine if $Mn(CH_3COO)_2{\cdot}4H_2O$ or $MnCO_3$ performed a catalytic function, a comparative experiment was executed, 1.5 g $MnCO_3$ was added to 40 mL ethanol maintained at 600 °C for 12 h, and the SEM image of the product is shown in Fig. 4f, we can only see carbon spheres in the picture, which indicated that $MnCO_3$ do not play a role to assist the generation of olivary carbon.

Figure 5a shows the typical TGA curve of the $Mn(CH_3COO)_2{\cdot}4H_2O$ sample. The first stage was from room temperature to about 130 °C which resulted from the evaporation of crystal water, the second loss occurred at about 300 °C, it can attributed to the decomposition of manganese acetate. The residual weight in TGA is about 30%, which implies that the residue is MnO. However, the $Mn(CH_3COO)_2{\cdot}4H_2O$ decomposes into $MnCO_3$ under the autoclave condition, which reveals that the autoclave offered a special reaction circumstance; high temperature and high pressure to assist the formation of the olivary carbon.

We can clearly see from Fig. 5b that there are some carbon spheres with different sizes. The lesser particles (1–3 μm) adhere to the bigger spheres (4–6 μm), and then the olivary carbons are formed with the growing of the carbon spheres (Fig. 5c). We can also explain the formation mechanism of such olivary carbon by Fig. 6. First, the $Mn(CH_3COO)_2{\cdot}4H_2O$ decomposes into $MnCO_3$, water and carbon fragments, and the ethanol turns into carbon spheres with different size at high temperature. Then two small size carbon spheres adhere to the opposite poles of a big one under the autoclave pressure and high temperature. With the assist of the carbon fragments, the carbon spheres fuse together and grow into pretty olivary particles slowly (as the route a shown in Fig. 6). With no doubt, not all of the carbon spheres could grow into pretty olivary particles in such a growth process, the SEM image in Fig. 5d shows some defective carbon particles, and the routes b–d in Fig. 6 reveal their growing process. On the other hand, these defective carbon particles also demonstrate the

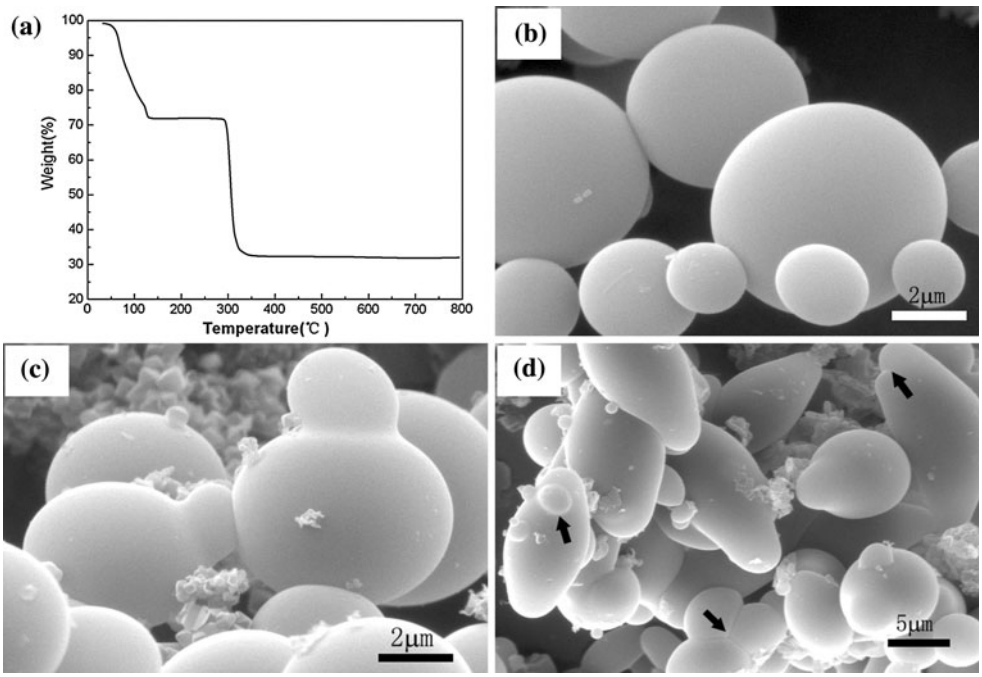

Fig. 5 **a** TGA curve for the $Mn(CH_3COO)_2{\cdot}4H_2O$ sample in N_2, **b** SEM image of carbon spheres, **c** olivary particles in growing, **d** some defective olivary particles

formation process we proposed well. The olivary carbon connects with the carbon spheres closely, and the role of the manganese acetate is to conduct the carbon spheres to adhere to their right places, which grow into pretty olivary particles. The carbon fragments generated by the manganese acetate fill in the interstices between carbon spheres, and assist the olivary particles become smooth.

Figure 7 shows the FTIR spectra of the as-prepared products. The strong characteristic peak at 3445 cm^{-1} attributed to the –OH bending vibration, which implies the existence of residual hydroxyl groups. The peaks at 2920 and 2850 cm^{-1} due to the stretching vibration of $–CH_2–$OH, and the absorption peak at 1120 cm^{-1} corresponds to the C–OH stretching and –OH bending vibrations. The infrared spectrum peaked at 1636 cm^{-1} is due to the stretching vibration of carboxyl groups. These results indicate that there are a large number of residues hydroxyl groups on the surface of the as-prepared olivary carbon due

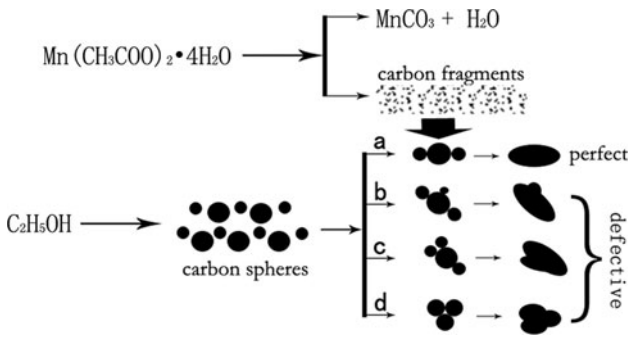

Fig. 6 Schematic illustrations for the possible formation process of olivary particle

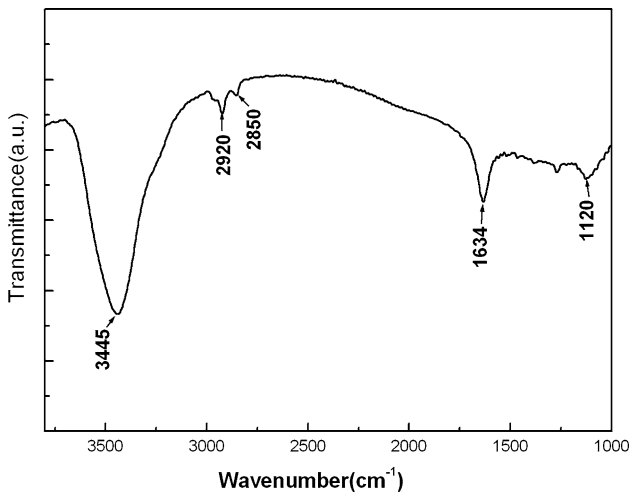

Fig. 7 FTIR spectra of as-obtained products

to an incomplete carbonization, and they play important roles in the formation process of the olivary carbon [21, 22]. The hydroxyl groups are able to absorb the carbon spheres together; this also gives a convincing support to the formation process.

Conclusions

In conclusion, a new economical route was found to prepare olivary carbon by the pyrolysis of ethanol with manganese acetate as the promoter in an autoclave at 600 °C for 12 h. The olivary carbon microparticles have a diameter of 4–6 μm at the middle and a length 8–12 μm.

Manganese acetate plays a vital role in the formation of olivary carbon. A possible schematic illustration was put forward to explain the formation of the olivary carbon. The olivary carbon not only used as templates for the synthesis of other materials but also has potential applications in catalyst carrier, gas storage media and electrode materials and so on.

Acknowledgement This work was financially supported by the Natural Science Union Foundations of China and Guangdong Province (U0734005) and Natural Nature Science Foundation of China (20906037) and the Fundamental Research Funds for the Central Universities (21610102).

References

1. Kroto HW, Heath JR, O'Brien SC, Curl RF, Smalley RE (1985) Nature 318:162
2. Iijima S (1991) Nature 354:56
3. Bandow S, Asaka S, Saito Y, Rao AM, Grigorian L, Richer E, Eklund PC (1998) Phys Rev Lett 80:3779
4. Fan SS, Chapline MG, Franklin NR, Tombler TW, Cassell AM, Dai HJ (1999) Science 283:512
5. Moreno JMC, Yoshimura M (2001) J Am Chem Soc 123:741
6. Basavalingu B, Byrappa K, Yoshimura M, Madhusudan P, Dayananda AS (2006) J Mater Sci 41:1465. doi:10.1007/s10853-006-7487-6
7. Demazeau G (2008) J Mater Sci 43:2104. doi:10.1007/s10853-007-2024-9
8. Ma XC, Xu F, Chen LY, Zhang YG, Zhang ZD, Qian J, Qian YT (2006) Carbon 44:2861
9. Ni YB, Shao MW, Tong YH, Qian GX, Wei XW (2005) J Solid State Chem 178:908
10. Liu JW, Lin WJ, Chen XY, Zhang SY, Li FQ, Qian YT (2004) Carbon 42:669
11. Jiang Y, Wu Y, Zhang SY, Xu CY, Yu WC, Xie Y, Qian YT (2000) J Am Chem Soc 122:12383
12. Liu JW, Shao MW, Chen XY, Yu WC, Liu XM, Qian YT (2003) J Am Chem Soc 125:8088
13. Mi YZ, Liu YL, Yuan DS, Zhang JX, Xiao Y (2005) J Mater Sci 40:3635. doi:10.1007/s10853-005-0489-y
14. Luo T, Liu JW, Chen LY, Zeng SY, Qian YT (2005) Carbon 43:755
15. Luo T, Chen LY, Bao KY, Yu WC, Qian YT (2006) Carbon 44:2844
16. Xiao Y, Liu YL, Mi YZ, Yuan DS, Zhang JX, Cheng LQ (2005) Chem Lett 34:1422
17. Xiao Y, Liu YL, Cheng LQ, Yuan DS, Zhang JX, Gu YL, Sun GH (2006) Carbon 44:1589
18. Luo T, Gao LS, Liu JW, Chen LY, Shen JM, Wang LC, Qian YT (2005) J Phys Chem B 109:15272
19. Ma XC, XuF DuY, Chen LY, Zhang ZD (2006) Carbon 44:179
20. Pol VG, Calderon-Moreno JM, Thiyagarajan P (2009) Ind Eng Chem Res 48:5691
21. Zheng MT, Liu YL, Xiao Y, Zhu Y, Guan Q, Yuan DS, Zhang JX (2009) J Phys Chem C 113:8455
22. Zheng MT, Liu YL, Zhao S, He WQ, Xiao Y, Yuan DS (2010) Inorg Chem 49:8674